ISSN 1070-3632, Russian Journal of General Chemistry, 2021, Vol. 91, No. 5, pp. 890–896. © Pleiades Publishing, Ltd., 2021.

New Cr(III), Mn(II), Fe(III), Co(II), Ni(II), Zn(II), Cd(II), and Hg(II) Gibberellate Complexes: Synthesis, Structure, and Inhibitory Activity Against COVID-19 Protease

Moamen S. Refat[a,*], T. Altalhi[a], Safyah B. Bakare[b], Ghaferah H. Al-Hazmi[c], and Kehkashan Alam[d]

[a] *Department of Chemistry, College of Science, Taif University, P.O. Box 11099, Taif, 21944 Saudi Arabia*
[b] *Faculty of Education, Shaqra University, Al Muzahimiyah, Shaqra, Riyadh Province, P.O. Box 205, 11972 Saudi Arabia*
[c] *Department of Chemistry, College of Science, Princess Nourah bint Abdulrahman University, Riyadh, 11671 Saudi Arabia*
[d] *Department of Chemistry, Faculty of Science, Aligarh Muslim University, Aligarh, 202002 India*
**e-mail: msrefat@yahoo.com; moamen@tu.edu.sa*

Received December 29, 2020; revised February 8, 2021; accepted May 6, 2021

Abstract—Transition metals such as Cr(III), Mn(II), Fe(III), Co(II), Ni(II), Zn(II), Cd(II), and Hg(II) have been reacted with gibberellic acid (HGA) to give novel complexes, and those have been characterized by physical, spectral and analytical methods. The plant hormone gibberellate acts as a deprotonated bidentate ligand in the complexation reaction with central metal ions in the ratio 1 : 2 (M^{n+} : GA). The complexes $[M(GA)_2(H_2O)_2]$, where [M = Mn(II), Co(II), and Ni(II)] form octahedral structures, while $[M(GA)_2]$ complexes [M = Zn(II), Cd(II), and Hg(II)] display four-coordination geometry. The octahedral structures of Cr(III) and Fe(III) complexes are characterized by the general formula $[M(GA)_2(H_2O)(Cl)]$. Computational study carried out has determined possible interactions of the complexes with COVID-19 (6LU7).

Keywords: gibberellic acid; chelation; transition metals, COVID-19

DOI: 10.1134/S1070363221050194

INTRODUCTION

Gibberellic acid (HGA) is a tetra-terpenoid compound [1] that acts as a plant hormone stimulating plants growth and development. Understanding the appropriate mechanism of HGA transport and action upon plant growth, flower development, sexual expression, grain development, and seeds germination is the objective of extensive research [2, 3].

So far there are no publications on metals chelation with gibberellic acid, except our published paper devoted to the structural, morphological and biological properties of $(NH_4)_2[PtL(H_2O)_2]Cl_3\cdot 2H_2O$, $[AuLCl_2]\cdot 3H_2O$, $[RuL(NH_3)_2Cl_2]\cdot 6H_2O$, $[VL(NH_3)_2Cl_2]\cdot 2H_2O$, and $[SeOL(H_2O)Cl]\cdot 3H_2O$ (where L: GA) complexes with the ions of Pt(II), Au(III), Ru(III), V(III), and Se(IV) [4]. In continuation of that research, we report here new transition metals Cr(III), Mn(II), Fe(III), Co(II), Ni(II), Zn(II), Cd(II), and Hg(II) complexes with gibberellic acid. Influence of different ions nature upon chelation is discussed. Interactions of the complexes with COVID-19 protease (6LU7) by means of molecular docking are considered.

EXPERIMENTAL

Gibberellic acid and metal chlorides were received from Sigma–Aldrich Chemical Corporation, St. Louis, Mo, USA. Those were of analytical grade and used without further purification.

Melting points of all synthesized complexes were measured on a MPS10-120 melting point apparatus. Molar conductance of the complexes was measured in DMSO (1.0×10^{-3} mol/dm^3) solutions at 30°C on a Jenway 4010 conductivity meter. Magnetic susceptibility measurements were performed on a SHERWOOD SCIENTIFIC magnetic susceptibility balance. IR spectra (KBr discs) were recorded on a Bruker FTIR spectrophotometer. UV-Vis spectra were recorded on a UV2 Unicam UV/Vis spectrophotometer. ^{1}H NMR spectra were measured on a Bruker DRX-250 spectrometer (600 MHz) using DMSO-d_6 as a solvent. ESR spectra were measured on a JES-FE2XG EPR spectrometer. Elemental analysis of the complexes was carried out on a PerkinElmer 2400 organic elemental analyzer. Percentage of the metal ions was determined by the gravimetric method.

The complexes of Cr(III), Mn(II), Fe(III), Co(II), Ni(II), Zn(II), Cd(II), and Hg(II) with gibberellic acid were prepared by the general procedure. The desired anhydrous metal chloride salt (1 mmol) was dissolved in 20 mL of distilled water, and the solution was slowly added to 20 mL of 2 mmol methanol (95%) solution of gibberellic acid upon magnetic stirring. The pH of the reaction mixture was maintained ca 7–8 by adding 10% alcoholic ammonia solution, and the mixture was refluxed for ca 2 h. The precipitate was filtered off while hot and washed with hot methanol, diethyl ether and dried over anhydrous $CaCl_2$ in a vacuum desiccator to give the corresponding solid complex.

[Cr(GA)$_2$(H$_2$O)(Cl)]. Dark blue, yield 66%, mp 245°C, Λ_m = 12 Ω^{-1} cm^2 mol^{-1}. IR spectrum, ν, cm^{-1}: 1604 ν_{as}(COO), 1331 ν_s(COO). Found, %: C 57.21; H 5.49; M 6.46. $C_{38}H_{44}ClCrO_{13}$. Calculated, %: C 57.32; H 5.57; Cr 6.53. *M* 796.20.

[Fe(GA)$_2$(H$_2$O)(Cl)]. Reddish brown, yield 69%, mp 272°C, Λ_m = 17 Ω^{-1} cm^2 mol^{-1}. IR spectrum, ν, cm^{-1}: 1590 ν_{as}(COO), 1330 ν_s(COO). Found, %: C 57.01; H 5.50; M 6.93. $C_{38}H_{44}ClFeO_{13}$. Calculated, %: C 57.05; H 5.54; Fe 6.98. *M* 800.05.

[Mn(GA)$_2$(H$_2$O)$_2$]. Light brown, yield 71%, mp 264°C, Λ_m = 10 Ω^{-1} cm^2 mol^{-1}. IR spectrum, ν, cm^{-1}: 1565 ν_{as}(COO), 1331 ν_s(COO). Found, %: C 58.32; H 5.88; M 6.97. $C_{38}H_{46}MnO_{14}$. Calculated, %: C 58.39; H 5.93; Mn 7.03. *M* 781.71.

[Co(GA)$_2$(H$_2$O)$_2$]. Red, yield 68%, mp 257°C, Λ_m = 11 Ω^{-1} cm^2 mol^{-1}. IR spectrum, ν, cm^{-1}: 1612 ν_{as}(COO), 1379 ν_s(COO). Found, %: C 58.04; H 5.87; M 7.44. $C_{38}H_{46}CoO_{14}$. Calculated, %: C 58.09; H 5.90; Co 7.50. *M* 785.71.

[Ni(GA)$_2$(H$_2$O)$_2$]. Green, yield 74%, mp 266°C, Λ_m = 14 Ω^{-1} cm^2 mol^{-1}. IR spectrum, ν, cm^{-1}: 1612 ν_{as}(COO), 1332 ν_s(COO). Found, %: C 58.07; H 5.85; M 7.40. $C_{38}H_{46}NiO_{14}$. Calculated, %: C 58.11; H 5.90; Ni 7.47. *M* 785.47.

[Zn(GA)$_2$]. White, yield 64%, mp 283°C, Λ_m = 9 Ω^{-1} cm^2 mol^{-1}. IR spectrum, ν, cm^{-1}: 1621 ν_{as}(COO), 1333 ν_s(COO). Found, %: C 60.21; H 5.56; M 8.46. $C_{38}H_{42}O_{12}Zn$. Calculated, %: C 60.36; H 5.60; Zn 8.65. *M* 756.12.

[Cd(GA)$_2$]. White, yield 66%, mp 289°C, Λ_m = 13 Ω^{-1} cm^2 mol^{-1}. IR spectrum, ν, cm^{-1}: 1561 ν_{as}(COO), 1330 ν_s(COO). Found, %: C 56.77; H 5.20; M 13.78. $C_{38}H_{42}CdO_{12}$. Calculated, %: C 56.83; H 5.27; Cd 14.00. *M* 803.16.

[Hg(GA)$_2$]. White, yield 65%, mp 222°C, Λ_m = 11 Ω^{-1} cm^2 mol^{-1}. IR spectrum, ν, cm^{-1}: 1556 ν_{as}(COO), 1329 ν_s(COO). Found, %: C 51.19; H 4.72; M 22.43. $C_{38}H_{42}HgO_{12}$. Calculated, %: C 51.21; H 4.75; Hg 22.50. *M* 891.33.

RESULTS AND DISCUSSION

The synthesized Cr(III), Mn(II), Fe(III), Co(II), Ni(II), Zn(II), Cd(II), and Hg(II) complexes were insoluble in common organic solvents such as methanol, ethanol, chloroform, or benzene, but soluble in DMSO and DMF. Molar conductance values of the complexes in DMSO were low (9–17 Ω^{-1} cm^2 mol^{-1}) indicating those as non-electrolytes [5]. The physical and analytical data accumulated for the complexes were in good agreement with the proposed molecular formulae viz. [M(GA)$_2$(H$_2$O)$_2$] [where M = Mn(II), Co(II), and Ni(II)], [M(GA)$_2$] [where M = Zn(II), Cd(II), and Hg(II)] and [M(GA)$_2$(H$_2$O)(Cl)] [where M = Cr(III) and Fe(III)].

IR spectra of free gibberellic acid and its complexes are listed in Table 1. In case of the complexes, the stretching vibrations ν(O–H) bands were recorded in the range of 3330–3396 cm^{-1} due to deprotonation of the carboxylic group and its involvement in complexation with the central metal ions. The characteristic band of ν(C=O) at 1750 cm^{-1} of the free ligand was recorded at the same frequency as in IR spectra of the complexes. The band at 1660 cm^{-1} assigned to the ν(C=O) of free HGA was absent in the spectra of the synthesized complexes. There were recorded two new vibration bands in the ranges of 1621–1556 and 1379–1329 cm^{-1} assigned to ν_{as}(C=O) and ν_a(C=O) of the carboxylate group. The calculated values of [Δν(COO)] (Table 2) that were in the range of 288–227 cm^{-1} confirmed the bidentate coordination modes [5–7]. The new vibration bands in the range of 644–537 cm^{-1} were assigned to ν(M–O) [6].

UV-Vis spectra bands recorded for HGA in the range of 200–300 nm were assigned to π–π* transitions. The broad band observed in the visible region of the complexes spectra was attributed to *d–d* transitions of the metal ions.

Electronic spectrum of Cr(III) complex exhibited the spin transitions at 393, 451 and 566 nm due to $^4A_{2g} \rightarrow {}^4T_{1g}$ (P) (ν_3), $^4A_{2g} \rightarrow {}^4T_{1g}$ (F) (ν_2), and $^4A_{2g} \rightarrow {}^4T_{2g}$ (F) (ν_1), respectively, and indicated an octahedral geometry of the complex, which was supported by ν_2 to ν_1 ratio of

Table 1. IR spectral data (cm^{-1}) for gibberellic acid and its complexes

HGA	Cr(III)	Mn(II)	Fe(III)	Co(II)	Ni(II)	Zn(II)	Cd(II)	Hg(II)	Assignments
3450	3393	3390	3373	3330	3375	3370	3396	3380	ν(OH)
3380									
2970	2936	2934	2938	2937	2935	2935	2936	2936	$\nu_{as}(CH) + \nu_s(CH)$
2930									
–	1604	1565	1590	1612	1612	1621	1561	1556	ν_{as} (OCO)
1750	1756	1754	1757	1756	1754	1756	1756	1748	ν(C=O) carbonyl
1660	–	–	–	–	–	–	–	–	ν(CO) carboxylic
1455	1550	1411	1330	1379	1406	1406	1413	1407	$\delta(CH_2) + \nu_s(OCO)$
1416	1426	1331			1332	1333	1330	1329	ν(C=C)
1382	1331								
1258	1253	1291	1255	1170	1252	1291	1254	1257	ν(C–O)
	1165	1253	1163		1166	1254	1165	1173	$\rho_w(CH_2)$
		1170				1169			
1094	1101	1094	1102	1098	1100	1094	1099	1100	$\nu_{as}(CC)$
	1045	1048	1042	1049	1045	1047	1043	1026	
950	993	987	973	945	946	945	946	972	ν_s (CC)
853	891	886	892	889	889	888	890	891	δ(CC) + δ(OCO)
–	554	559	602		613	640	573	591	ρ_w(OCO) + ν(M–O)
			565	644		562		537	

Table 2. IR spectral data for the carboxylate group of the complexes

Complexes	ν_{as}, cm^{-1}	ν_s, cm^{-1}	$\Delta\nu = \nu_{as} - \nu_s$	Bonding mode
Cr(III)	1604	1331	273	Bidentate
Mn(II)	1565	1331	234	Bidentate
Fe(III)	1590	1330	260	Bidentate
Co(II)	1612	1379	233	Bidentate
Ni(II)	1612	1332	280	Bidentate
Zn(II)	1621	1333	288	Bidentate
Cd(II)	1561	1330	231	Bidentate
Hg(II)	1556	1329	227	Bidentate

1.25 [7]. At room temperature magnetic moment of the complex was measured to be 3.61 B.M., close to the spin only value suggesting an octahedral geometry around chromium ion [8].

The spectrum of Mn(II) demonstrated the bands at 806 and 823 nm of the electronic transfers $^6A_{1g} \rightarrow {}^4T_{2g}(G)$ and $^6A_{1g} \rightarrow {}^4T_{1g}(G)$, respectively, and proposed the octahedral structure of Mn(II) ion [7]. The effective magnetic moment value of the complex was 5.92 B.M.

The spectrum of Fe(III) complex demonstrated the bands at 652 nm (ν_1), 470 nm (ν_2) and 447 nm (ν_3) assigned to the transitions $^6A_{1g} \rightarrow {}^4T_{1g}$ (D), $^6A_{1g} \rightarrow {}^4T_{1g}$ and $^6A_{1g} \rightarrow {}^4T_{2g}$, respectively. The magnetic moment value of 5.55 B.M. confirmed the high spin octahedral geometry of the complex [7].

The spectrum of Co(II) complex contained four bands at 308, 381, 680, and 820 nm attributed to C–T mixed with $^4T_{1g}(F) \rightarrow {}^4T_{1g}(P)$, $^4T_{1g}(F) \rightarrow {}^4A_{2g}$ and $^4T_{1g}(F) \rightarrow {}^4T_{2g}(F)$ respectively assigned to octahedral Co(II) ion [9–12], which was confirmed by the effective magnetic moment value of 4.75 B.M. assigned to three unpaired electrons per Co(II) ion.

The spectrum of Ni(II) complex exhibited three electronic transition bands at 811, 611 and 386 nm assigned to $^3A_{2g} \rightarrow {}^3T_{2g}(F)$ (ν_1), $^3A_{2g}(F) \rightarrow {}^3T_{1g}(F)$ (ν_2) and $^3A_{2g}(F) \rightarrow {}^3T_{2g}(P)$ (ν_3) transitions, respectively,

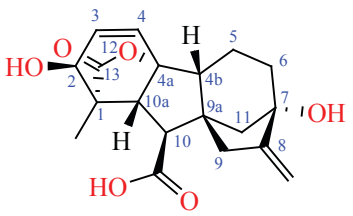

Fig. 1. Molecular structure of gibberellic acid (HGA).

attributed to octahedral geometry [7]. The μ_{eff} value of 3.20 B.M. corresponded to two unpaired electrons per Ni(II) ion with the ideal six-coordinated configuration. The ratio of ν_2/ν_1 (1.32) supported the octahedral structure of the complex [7, 8].

The Zn(II), Cd(II), and Hg(II) complexes were determined to be diamagnetic demonstrating no d-d bands and their spectra demonstrated only charge transfer bands.

^{1}H NMR spectra. *Gibberellic acid.* ^{1}H NMR spectrum, δ, ppm: 1.07 s (3H, CH_3), 1.66 d (1H, J = 6.6 Hz, $C_{11}H$), 1.71–1.74 m (3H, $C_{4b}H$, C_5H, C_6H), 1.84 d (1H, J = 6.6 Hz, $C_{11}H$), 1.86 m (1H, C_6H), 1.91 m (1H, C_5H), 2.11 d (1H, J = 16.2 Hz, C_9H), 2.17 d (1H, J = 16.2 Hz, C_9H), 2.48 d (1H, J = 10.6 Hz, $C_{10a}H$), 3.02 d (1H, J = 10.2 Hz, $C_{10}H$), 3.55 d (1H, J = 3.16 Hz, C_2H), 3.87 s (1H, C_7OH), 4.85 s (1H, C_2OH), 5.10 d (1H, J = 8.16 Hz, $C_{methylene}H$), 5.56 d (1H, J = 8.12 Hz, $C_{methylene}H$), 5.78 m (1H, C_3H), 6.32 d (1H, J = 9.36 Hz, C_4H), 12.55 sb (1H, COOH).

Cd(II) complex. ^{1}H NMR spectrum, δ, ppm: 1.02 s (3H, CH_3), 1.57 d (1H, J = 6.6 Hz, $C_{11}H$), 1.61–1.63 m (3H, $C_{4b}H$, C_5H, C_6H), 1.76 d (1H, J = 6.6 Hz, $C_{11}H$), 1.83 m (1H, C_6H), 2.03 m (1H, C_5H), 2.11 d (1H, J = 11.96 Hz, C_9H), 2.38 d (1H, J = 6.8 Hz, C_9H), 2.46 d (1H, J = 10.68 Hz, $C_{10a}H$), 3.01 d (1H, J = 10.6 Hz, $C_{10}H$), 3.12 d (1H, J = 13.64 Hz, C_2H), 4.78 m (1H, C_3H), 5.03 s (1H, C_7OH), 5.61 s (1H, C_2OH), 5.71 d (1H, J = 3.56 Hz, $C_{methylene}H$), 5.73 d (1H, J = 3.60Hz, $C_{methylene}H$), 6.26 d (1H, J = 9.36 Hz, C_4H).

The combination of microanalytical and spectroscopic characteristics of the gibberellic acid (Fig. 1) and its complexes (Fig. 2) indicated that the deprotonated acid acted as a bidentate chelate towards the studied metal ions giving the complexes $[M(GA)_2(H_2O)_2]$ (where M = Mn(II), Co(II), and Ni(II)], $[M(GA)_2]$ [where M = Zn(II), Cd(II), and Hg(II)], and $[M(GA)_2(H_2O)(Cl)]$ [where M = Cr(III) and Fe(III)] (Fig. 2).

Molecular docking. In this study Auto Dock (ADT) programming was used for the docking procedure. Optimization of the ligand was performed prior to docking by Avogadro version 1.2. The structure of COVID-19 protease (6LU7) was downloaded from the Protein Data Bank (http://www.rcsb.org) [10]. In the AutoDock Tools, the 6LU7 was prepared for docking by adding polar hydrogen bonds and Kollman & Gasteiger charges. We characterized the grid size for the receptor, and Lamarckian Genetic Algorithm was appointed to do the molecular docking as portrayed in this study. The

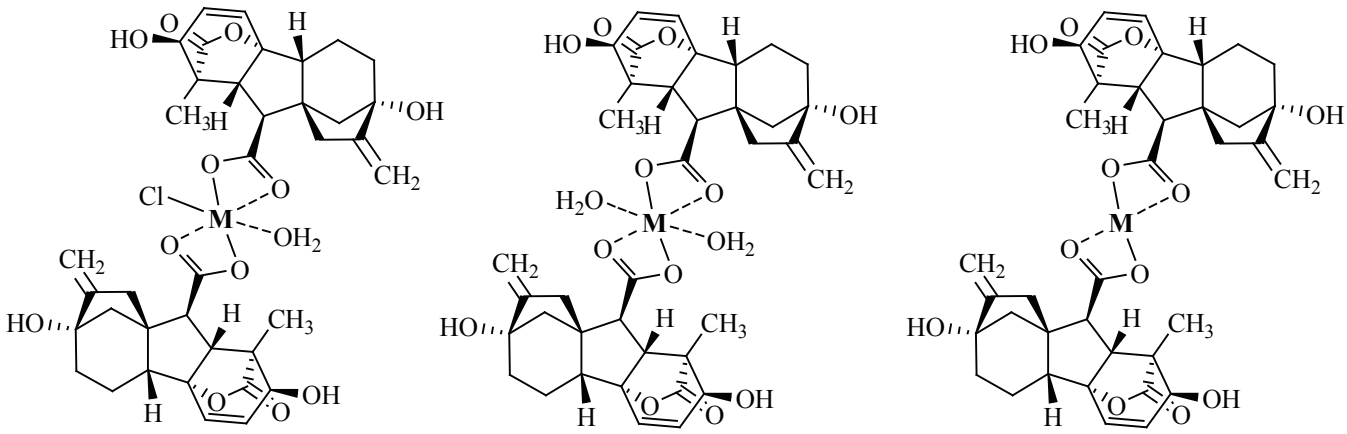

M = Fe(III) or Cr(III) M = Mn(II), Co(II), or Ni(II) M = Hg(II), Zn(II), or Cd(II)

Fig. 2. Proposed structures of gibberellic acid complexes with metals.

Table 3. Docking parameters

Complex	Binding free energy, kcal/mol	Total intermolecular energy, kcal/mol	Inhibition constant, μM	Interacting amino acids
Cd(II)	–7.72	–9.37	2.190	Glu166, Val3, Met49
Hg(II)	–7.27	–8.92	4.690	Phe140, Leu141, Asn142, Glu166, Asn119
Cr(III)	–6.77	–8.69	10.850	Asn142, Val3, Glu166, Gln189
Mn(II)	–9.48	–11.67	0.112	Ala193, Gly183, Thr190, Arg188, Gly179, Pro184
Fe(III)	–5.89	–7.98	47.960	Glu166, Val3, Leu4, Asn142, Leu141
Co(II)	–8.34	–10.54	0.766	Val3, Met49, Leu141, Asn142, Asn119, Thr24
Ni(II)	–7.41	–9.80	3.710	Met49, Gln189, Leu4, Val3, Ala2,
Zn(II)	–7.76	–9.55	2.050	Ala194, Asp197, Lys137, Leu286

output obtained was further analyzed and visualized utilizing the discovery studio program.

It was apparent that the complexes under study might have one-of-a-kind effects on COVID-19 protease. The active sites of 6LU7 were revealed from the PDB files using discovery studio (Table 3). The helical models of the compounds with 6LU7 are presented in Fig. 3, and the most conceivable docking present among 6LU7 and various compounds and interactions with different amino acids are represented in Fig. 4. The highest binding energy

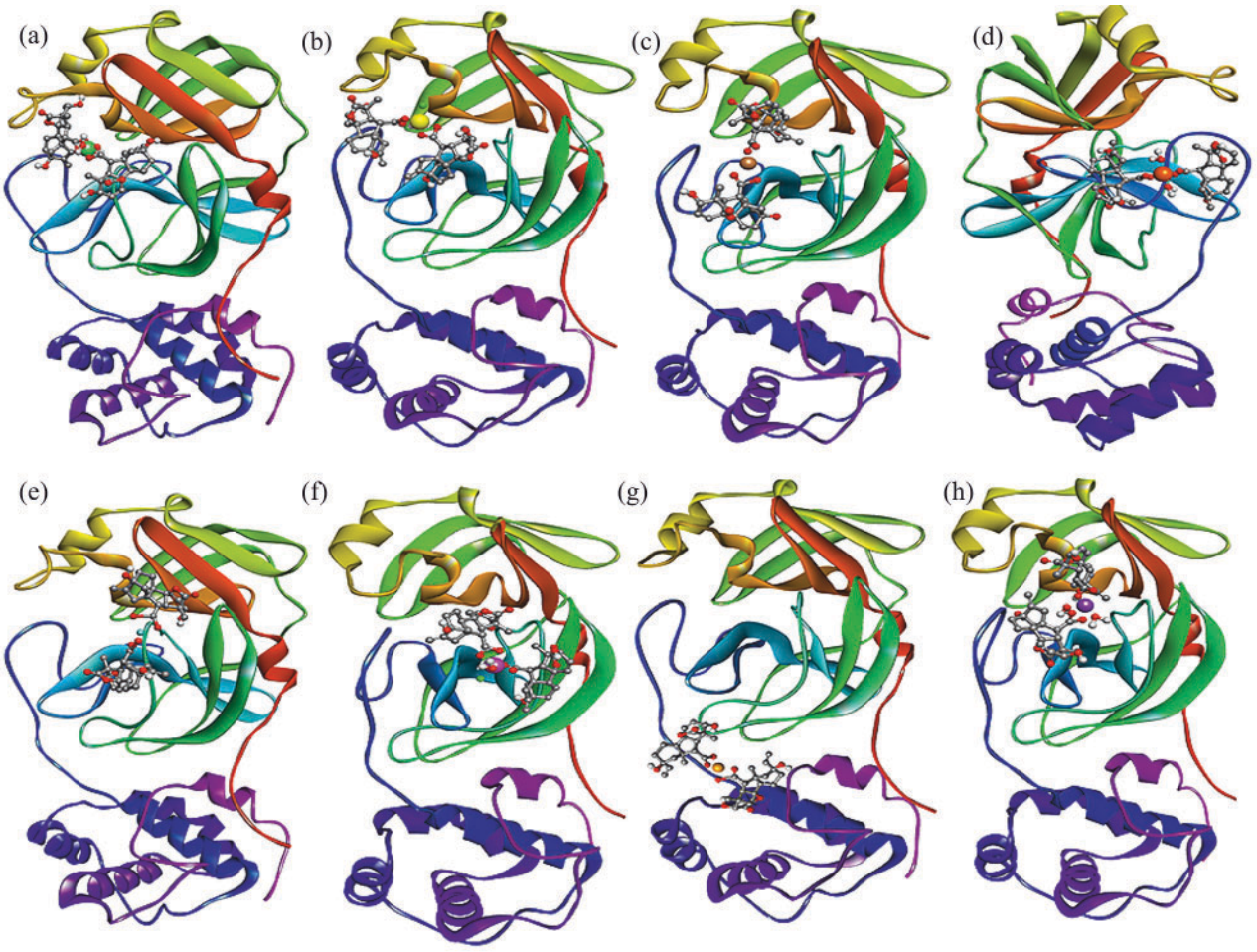

Fig. 3. Helical models of giberelette complexes with (a) Co(II); (b) Cr(III); (c) Cd(II); (d) Mn(II); (e) Hg(II); (f) Fe(III); (g) Zn(II), and (h) Ni(II).

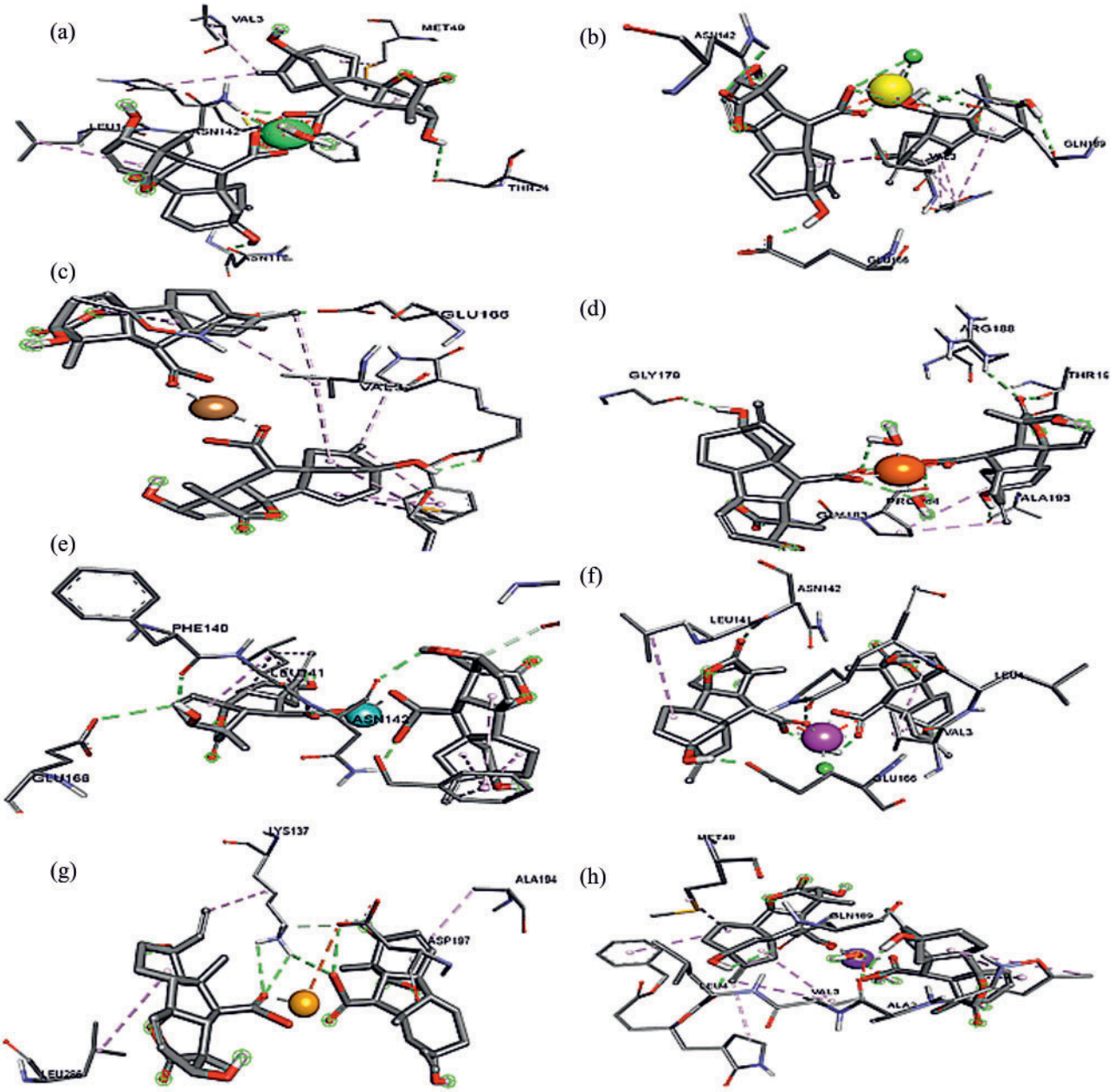

Fig. 4. Molecular docking poses of the gibberellate complexes with COVID-19 protease (6LU7) representing interactions with amino acids: (a) Co(II); (b) Cr(III); (c) Cd(II); (d) Mn(II); (e) Hg(II); (f) Fe(III); (g) Zn(II), and (h) Ni(II).

was determined for Mn(II) gibberellate complex (Table 3), which might act as a potential inhibitor of 6LU7.

FUNDING

Taif University Researches Supporting Project number (TURSP-2020/01), Taif University, Taif, Saudi Arabia.

CONFLICT OF INTEREST

No conflict of interest was declared by the authors.

REFERENCES

1. Gupta, R., and Chakrabarty, S.K., *Plant Signaling & Behavior*, 2013, vol. 8, no. 9, p. 1, article no. e25504. https://doi.org/10.4161/psb.25504
2. Katsumi, M., Foard, D.E., and Phinney, B.O., *Plant Cell Physiol*., 1983, vol. 24, p. 379. https://doi.org/10.1093/oxfordjournals.pcp.a076527
3. Proebsting, W.M., Hedden, P., Lewis, M.J.,

Croker, S.J., and Proebsting, L.N., *Plant Physiol*., 1992, vol. 100, p. 1354. https://doi.org/10.1104/pp.100.3.1354

4. El-Sayed, M.Y., Fetooh, H., Refat, M.S., Eldaroti, H.H., Adam, A.M.A., and Saad, H.A., *J. Mol. Liquids*, 2019, vol. 296, p. 111895. https://doi.org/10.1016/j.molliq.2019.111895
5. Jin, Z., Du, X., Xu, Y., Deng, Y., Liu, M., Zhao, Y., Zhang, B., Li, X., Zhang, L., Peng, C., Duan, Y., Yu, J., Wang, L., Yang, K., Liu, F., Jiang, R., Yang, X., You, T., Liu, X., Yang, X., Bai, F., Liu, H., Liu, X., Guddat, L.W., Xu, W., Xiao, G., Qin, C., Shi, Z., Jiang, H., Rao, Z., and Yang, H., *Nature*, 2020, vol. 582, p. 289. https://doi.org/10.1038/s41586-020-2223-y
6. Alam, K. and Khan, I.M., *Org. Electron.*, 2018, vol. 63, p. 7. https://doi.org/10.1016/j.orgel.2018.08.037
7. Deacon, G.B. and Phillips, R.J., *Coord. Chem. Rev*., 1980, vol. 33, p. 227. https://doi.org/10.1016/S0010-8545(00)80455-5
8. Vogel's, *Textbook of Quantitative Chemical Analysis*, Longman Scientific and Technical Publishers, New York: John Wiley & Sons, 1989.
9. Nakamoto, K., *Infrared Spectra of Inorganic and Coordination Compounds*, New York: Wiley, 1970.
10. Lever, A.B.P., *Inorganic Electronic Spectroscopy*, Amsterdam: Elsevier, 1997, 2nd ed.
11. Figgis, B.N., *Introduction to Ligand Field Theory*, New York: Wiley, 1978.
12. Yongxiang, M., Zhengzhi, Z., Yun, M., and Gang, Z., *Inorg. Chim. Acta*, 1989, vol. 165, p. 185. https://doi.org/10.1016/S0020-1693(00)83237-5